

# Improvement of Automated Detection Method of Lacunar Infarcts in Brain MR Images

Yoshikazu Uchiyama, Ryujiro Yokoyama, Hiromichi Ando, Takahiko Asano, Hiroki Kato, Hiroyasu Yamakawa, Haruki Yamakawa, Takeshi Hara, Toru Iwama, Hiroaki Hoshi, and Hiroshi Fujita

**Abstract**—The detection of asymptomatic lacunar infarcts on magnetic resonance (MR) images are important tasks for radiologists to ensure the prevention of severe cerebral infarction. However, their accurate identification is often difficult task. Therefore, the purpose of this study is to develop a computer-aided diagnosis scheme for the detection of lacunar infarcts. Our database consisted of 1,143 T1- and 1,143 T2-weighted images obtained from 132 patients. We first segmented the cerebral region in the T1- weighted image by using a region growing technique. For identifying the initial lacunar infarcts candidates, white top-hat transform and multiple-phase binarization were then applied to the T2- weighted image. For eliminating false positives (FPs), we determined 12 features, i.e., the locations  $x$  and  $y$ , density differences in the T1- and T2-weighted images, nodular components (NC), and nodular & linear components (NLC) from a scale 1 to 4. The NCs and NLCs were obtained using filter bank technique. The rule-based scheme and a neural network with 12 features were employed as the first step for eliminating FPs. The modular classifier was then used for eliminating three typical sources of FPs. As a result, the sensitivity of the detection of lacunar infarcts was 96.8% with 0.30 FP per image. Our computerized scheme would assist radiologists in identifying lacunar infarcts on MR images. **Keywords:** *Lacunar infarcts, Magnetic resonance imaging (MRI), Computer-Aided Diagnosis, Modular classifier*

## I. INTRODUCTION

CEREBROVASCULAR diseases are the 3<sup>rd</sup> leading cause of death in Japan [1]. Therefore, a screening system for early detection of cerebral and cerebrovascular diseases, which is named *Brain Dock*, is widely performed in Japan. Because of the recent progress of magnetic resonance (MR) imaging, various types of cerebral diseases such as lacunar infarct, aneurysm, occlusion, and stenosis are detected in this system. In order to assist physicians' image interpretations as a "second opinion," we have been developing computer-aided diagnosis (CAD) schemes for the detection of lacunar infarcts [2, 3], aneurysms [4], and occlusions [5] in brain MR

Manuscript received April 2, 2007. This work was supported in part by a grant for the "Knowledge Cluster Creation Project" from the Ministry of Education, Culture, Sports, Science and Technology, Japan.

Y. Uchiyama, R. Yokoyama, T. Hara, and H. Fujita are with Dept. of Intelligent Image Information, Graduate School of Medicine, Gifu University, Yanagido 1-1, Gifu, 501-1194, Japan

T. Asano, H. Kato, and H. Hoshi are with Dept. of Radiology, Graduate School of Medicine, Gifu University, Japan.

H. Yamakawa and T. Iwama are with Dept. of Neurosurgery, Graduate School of Medicine, Gifu University, Japan.

H. Ando is with Dept. of Neurosurgery, Gifu Municipal Hospital, Japan.

H. Yamakawa is with Dept. of Emergency and Critical Care Medicine, Chuno-Kousei Hospital, Japan.

images.

The detection of asymptomatic lacunar infarcts is important because their presence indicates an increased risk of severe infarction [6]. However, accurate identification of lacunar infarcts on MR images is often hard to interpret for radiologists because of the difficulty in distinguishing the lacunar infarcts from certain normal tissue such as enlarged perivascular spaces [7]. Therefore, we have been developing CAD schemes for the detection of lacunar infarcts [2, 3]. Previously, Yokoyama *et al.* [2] developed two methods for the detection of isolated lacunar infarcts and lacunar infarcts adjacent to a cerebral ventricle. Uchiyama *et al.* [3] developed a method for eliminating false positives (FPs). The method was applied to 132 patient cases and the sensitivity of 96.8% with 0.71 FP was obtained. However, a new method for further elimination of FPs is necessary for the clinical application. In this study, we propose modular classifier technique as a new method for eliminating the remaining FPs. We also investigate the detection performance of our improved CAD scheme.

## II. MATERIAL

Our database consisted of 1,143 T1- and 1,143 T2-weighted images, and these were selected from 132 patients (mean age, 63.4 years; age range, 28-83 years). These images were acquired using a 1.5 T MR scanner (Signa Excite Twin Speed 1.5 T; GE Medical Systems) at the Gifu University Hospital (Gifu, Japan). The T1- and T2- weighted images were obtained using the fast spin-echo method with an effective echo time (TE) of 8 – 12 ms and 96 – 105 ms, respectively, and a repetition time (TR) of 300 – 500 ms and 3000 – 3500 ms, respectively. The matrix size of the axial image was  $512 \times 512$ , with a spatial resolution of 0.47 mm per pixel. The slice thickness was 5 mm and the slice gap was 2 mm.

We performed an observer study in order to determine the location of the lacunar infarcts on the images in our database. Two experienced neuroradiologists independently marked the location of the lacunar infarcts (3 – 15 mm, in diameter). In this study, a candidate that identified by both the neuro-radiologists was considered as a "lacunar infarct." The sensitivity for the detection of lacunar infarcts was calculated based on the location of the lacunar infarcts. On the other hand, the number of FPs per image was calculated based on the "non-lacunar slice." A slice was determined as non-lacunar

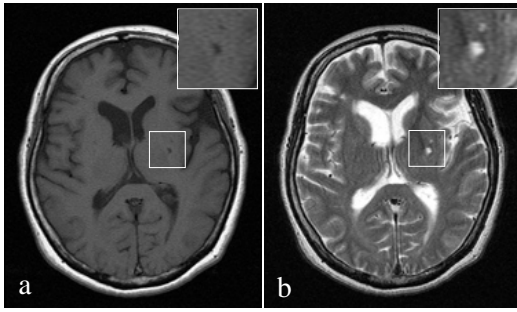


Fig.1 Example of lacunar infarct in (a) T1-weighted image and (b) T2-weighted image. Lacunar infarct has low intensity value in the T1-weighted image but high intensity value in the T2-weighted image.

when a point on the slice was not identified as a lacunar infarct by either of the two neuroradiologists. Our database included 93 lacunar infarcts and 1,063 non-lacunar slices. Figure 1 shows an example of lacunar infarct. Lacunar infarct has low intensity value in T1- weighted image and high intensity value in T2- weighted image.

### III. METHOD

#### A. Segmentation of the cerebral region

First, we segmented the cerebral region in T1- weighted image by using the region growing technique in order to avoid FPs outside the cerebral region. We calculated a histogram of the T1- weighted image. All pixel values of the brightest peak point in the histogram were set as seed points. The region was then grown by appending to each seed point when the difference between a point of interest and a value in the neighboring pixel was less than 15. Finally, the cerebral region was determined by eliminating the small regions with size-based feature analysis.

#### B. Determination of initial candidates for lacunar infarcts

The lacunar infarcts were classified into two types based on their location: the isolated lacunar infarcts (Fig.2 a) and lacunar infarcts adjacent to the cerebral ventricle (Fig.2 b). The former can be easily extracted using a simple threshold technique. However, it is difficult to extract the latter because the adjacent cerebral ventricle also has a high intensity value and its pixel value is similar to that of the lacunar infarcts. To overcome this issue, we applied the white top-hat transformation to the T2- weighted image in the segmented cerebral region. Figures 2c and 2d illustrate the image obtained on white top-hat transformation. As shown in these two figures, using this method, both of the isolated lacunar infarct and the lacunar infarct adjacent to the cerebral ventricle were enhanced. Thus, extraction of the lacunar infarcts adjacent to the cerebral ventricle is rendered easy using a thresholding technique.

By applying multiple-phase binarization to the image after white top-hat transformation, we determined the initial candidates for lacunar infarcts. In this procedure, thresholding techniques with several threshold values were

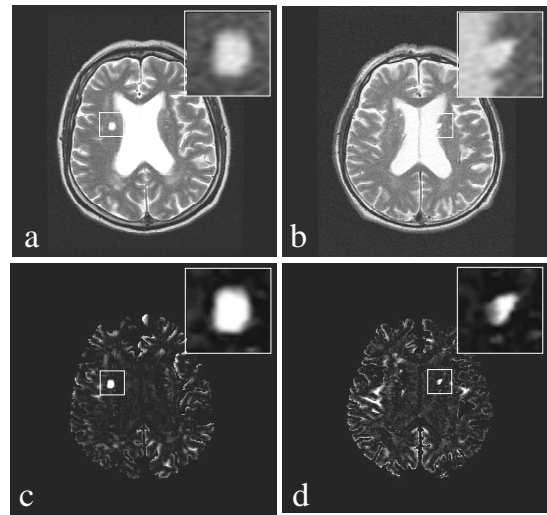


Fig.2 Efficacy of white top-hat transformation in the enhancement of lacunar infarcts. (a) T2-weighted image with an isolated lacunar infarct. (b) T2-weighted image with a lacunar infarct adjacent to cerebral ventricle. (c) The result image of (a) by using white top-hat transformation. (d) The result image of (c) by using white top-hat transformation.

applied to the T2-weighted image after white top-hat transformation. The thresholds for multiple-phase binarization were determined by increasing the pixel value from 55 to 205 at 15-pixel intervals. The total phase number of threshold values was 11. The size and degree of circularity were then calculated in each candidate region in the 11 binarized images. The regions were considered to be candidates for lacunar infarcts when the size was in the range of 33 to 285 pixels and the degree of circularity was greater than 0.59. The initial candidates for lacunar infarcts were determined by integrating the gravity centers of all candidates detected by multiple-phase binarization. If a candidate center appeared twice or more within a  $3 \times 3$  square region away from the gravity center of the candidate, was considered as a lacunar infarct candidate. On the other hand, if it appeared only once, it was regarded as FP and was eliminated.

#### C. Feature extraction

Using the techniques described in the previous sections, almost all lacunar infarcts were detected accurately. However, the candidates selected initially also included many FPs. For eliminating these, we determined 12 features in each initial candidate. These features included the locations  $x$  and  $y$ , density differences in the T2- and T1- weighted images, nodular components (NC) from a scale of 1 to 4, and nodular & linear components (NLC) from a scale of 1 to 4. The NCs and NLCs were obtained using a filter bank technique [8].

The locations  $x$  and  $y$  were defined based on the center of gravity in the candidate regions. The density difference on T1- and T2- weighted images were defined as the difference in the value between the average pixel value of the lacunar infarct region and the average pixel value of the peripheral region. Lacunar infarcts have low intensity values on T1-

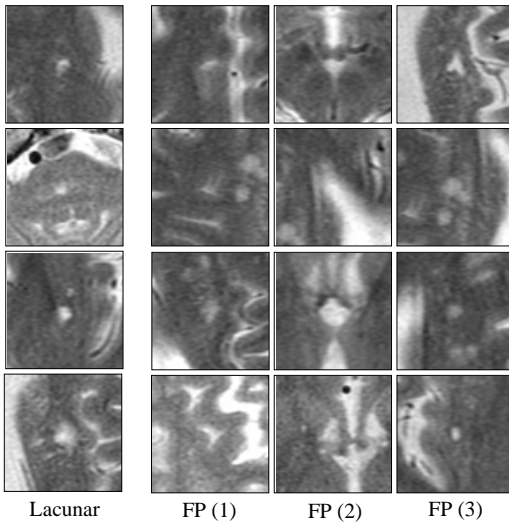


Fig.3 Example of lacunar infarcts and 3 typical sources of FPs. FP(1) indicates a part of the cerebral sulcus. FP(2) shows a part of the cerebral ventricle. FP(3) indicates enlarged perivascular space. The FP regions are located at the center of each figure.

weighted image and high intensity values in T2- weighted images. Thus, these features are important for distinguishing between lacunar infarcts and FPs. Analysis bank of the filter bank [8] yields the second derivative image in various sizes in the horizontal, vertical, and diagonal directions. Synthesis bank reconstructs the original image from these sub-images. The NC was defined based on the absolute value of the largest eigen-value of the Hessian matrix. On the other hand, the NLC was defined based on the absolute value of the smallest eigen- value of the Hessian matrix. NCs and NLCs from a scale of 1 to 4 are useful features for distinguishing between nodular patterns and line patterns.

#### D. Reduction of FPs with single classifier

The rule-based scheme with 12 features was employed as the first step in the elimination of FPs. In this scheme, we first calculated the maximum and minimum values of all lacunar infarcts detected in the initial step for identifying the lacunar candidates. The total 24 cutoff thresholds were then used for eliminating FPs, i.e., when a candidate was located outside the range determined by the cutoff thresholds in the feature space, the candidate was considered as FP.

A neural network (NN) with 12 features was employed as the second step in the elimination of FPs. A three-layer NN, which consisted of 12 input units, 3 hidden units, and 1 output unit, was used in this study. For training and testing the NN, we used holdout method. In this method, our database was randomly divided into two set: set A and set B. The former was first used for training and the latter for testing. This was then reversed, i.e., set B was used for training and set A for testing. The output value of the NN indicates the likelihood of lacunar infarcts. By changing the threshold level of the output, we can determine the performance for eliminating FPs. In this study, the threshold was set so as to keep the highest sensitivity for the detection of lacunar infarct.

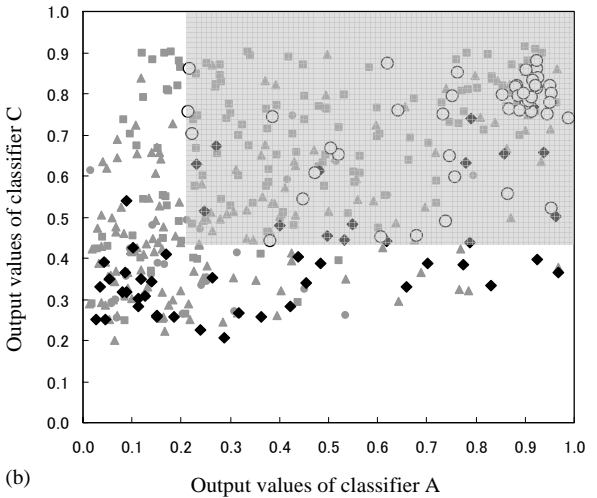
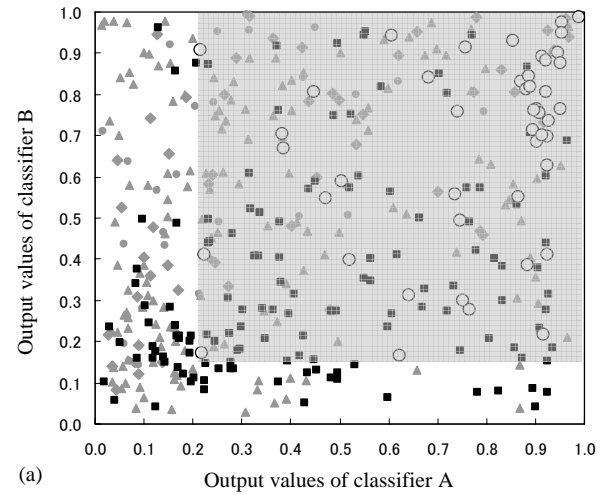


Fig.4 Relationship between output values from 3 classifiers. These were obtained from data set A. White circles indicate lacunar infarcts. Triangles indicate a part of the cerebral sulcus. Squares indicate a part of the cerebral ventricle. Diamonds indicates enlarged perivascular space. Gray circles indicate other FPs. In this scheme, the candidates outside gray range were considered as FPs

#### E. Reduction of FPs with modular classifier

Using the method described in the previous section, many FPs were eliminated. However, 753 FPs were obtained using this method. These FPs were classified into 4 types: a part of the cerebral sulcus, 47.9% (361/753); a part of the cerebral ventricle, 36.8% (277/753); the enlarged perivascular space, 11.2% (84/753); and others, 4.1% (31/753). Figure 3 shows the example of three major FP types. A part of cerebral sulcus can be distinguished from lacunar infarct by using shape-based feature because the difference in shape was shown between a part of cerebral sulcus and lacunar infarct. A part of the cerebral ventricle can be distinguished from lacunar infarct by using location-based feature because the cerebral ventricle is located at the center of brain. However, these FPs were not eliminated by using the single classifier described in the previous section. One reason is that the single classifier was trained for distinguishing lacunar infarcts from these different types of FPs. Because features obtained from these different types of FPs were located at different positions

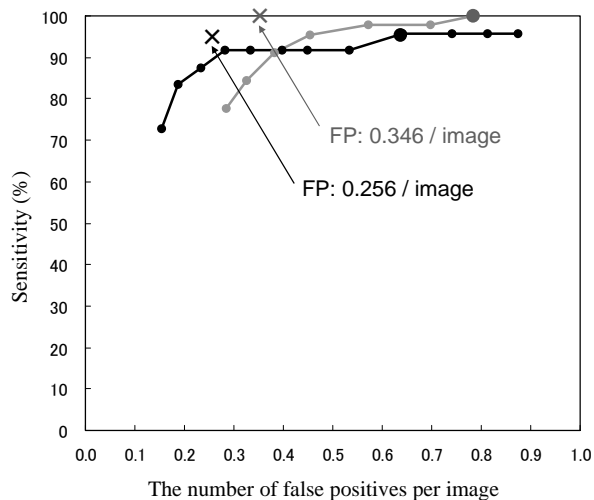


Fig.5 FROC curves for the overall performance of our CAD scheme in the detection of lacunar infarcts. The black and gray curves are the results of set A and set B, respectively. These curves were the results of reduction of FPs with single classifier. The cross marks (×) indicate the result of modular classifier. By using the modular classifier, many FPs were eliminated while keeping the same sensitivity.

in the feature space, some classifiers should be used for eliminating the specific type of FPs. In this study, three NNs were therefore employed for further elimination of FPs. The classifier A was trained for distinguishing a part of the cerebral sulcus and lacunar infarct. The classifier B was trained for distinguishing a part of cerebral ventricle and lacunar infarct. The classifier C was trained for distinguishing enlarged perivascular space and lacunar infarct.

#### IV. RESULT

We applied our computerized scheme to the T1- and T2-weighted images in our database. As the first step toward identifying the initial candidates for lacunar infarcts, 96.8% (90/93) lacunar infarcts were detected accurately with 6.88 (6771/1063) FPs per image. This result indicated that a combination of white top-hat transformation and multiple-phase binarization was useful in detection of lacunar infarct because almost all lacunar infarcts were accurately detected. However, many FPs were also detected.

For the elimination of FPs, the rule-based scheme and NN with 12 features were employed. This single classifier technique achieved the same sensitivity of 96.8% (90/93) with 0.71 (753/1063) FP per image. This result was obtained by averaging the results from set A and set B. Thus, 88.9% FPs were eliminated using this scheme. This result indicates that 12 features were useful in distinguishing between lacunar infarcts and FPs.

For further elimination of FPs, modular classifier technique was employed. Figure 4a shows relationship between output values from classifier A and classifier B. White circles and black triangles indicate lacunar infarcts and FPs due to a part of cerebral ventricle. The output values of classifier B obtained from a part of cerebral ventricle tended

to be small. Similarly, as shown in Fig.4b, the output values of classifier C obtained from enlarged perivascular space tended to be small. The result shows that each classifier can remove different types of FPs. For example, if a threshold of 0.17 is used for thresholding the output value from classifier B, 27.4% FPs due to cerebral ventricle can be removed without removing any lacunar infarct. If a threshold of 0.45 is used for thresholding the output value from classifier C, 68.0% FPs due to enlarged perivascular space can be removed without removing any lacunar infarct. Figure 5 shows the free-response receiver operating characteristic (FROC) curves, which were obtained from the results of set A and set B in the elimination of FPs with a single classifier. On the other hand, cross marks indicate the results with modular classifier technique. This result shows that our improved CAD scheme with modular classifier technique achieved the same sensitivity of 96.8% (90/93) with 0.30 (319/1063) FP per image.

#### V. CONCLUSION

We improved our CAD scheme for detection of lacunar infarcts on MRI images. Using modular classifier technique, the number of FPs was decreased from 0.71 to 0.30 per image while keeping the same sensitivity of 96.8%. Our improved CAD scheme would be useful in assisting radiologists in identifying lacunar infarcts on MRI images.

#### REFERENCES

- [1] Health and Welfare Statistics Association, "Vital Statistics of Japan 2003," volume 1, 300-301, 2003.
- [2] R. Yokoyama, X. Zhang, Y. Uchiyama, H. Fujita, T. Hara, X. Zhou, M. Kanematsu, T. Asano, H. Kondo, S. Goshima, H. Hoshi, T. Iwama, "Development of an automated method for detection of chronic lacunar infarct regions on brain MR images," *IEICE Trans. Inf. & Syst.*, E90-D(6), 943-954, 2007.
- [3] Y. Uchiyama, A. Matsui, R. Yokoyama, H. Fujita, T. Hara, X. Zhou, H. Ando, T. Iwama, T. Asano, H. Kato, and H. Hoshi, "CAD scheme for detection of lacunar infarcts in brain MR image," *International Journal of Computer Assisted Radiology and Surgery*, 1(1), 382-385, 2006.
- [4] Y. Uchiyama, H. Ando, R. Yokoyama, T. Hara, H. Fujita, and T. Iwama, "Computer-aided diagnosis scheme for detection of unruptured intracranial aneurysms in MR angiography". *Proc of IEEE Engineering in Medicine and Biology 27<sup>th</sup> Annual International Conference*, Shanghai, China, 3031-3034, 2005.
- [5] M. Yamauchi, Y. Uchiyama, R. Yokoyama, T. Hara, H. Fujita, H. Ando, H. Yamakawa, T. Iwama, and H. Hoshi, "Computerized scheme for detection of arterial occlusion in brain MRA images," *Proc of SPIE Medical Imaging, Computer-Aided Diagnosis*, 6514, 65142C-1-65142C-9, 2007.
- [6] S. Kobayashi, K. Okada, H. Koide, H. Bokura, and S. Yamaguchi, "Subcortical silent brain infarction as a risk factor for clinical stroke," *Stroke*, 28, 1932-1939, 1997.
- [7] H. Boukura, S. Kobayashi, and S. Yamaguchi, "Discrimination of silent lacunar infarction from enlarged Virchow-Robin spaces on brain magnetic resonance imaging and pathological study," *Journal of Neurology*, 245, 116-112, 1998.
- [8] R. Nakayama, Y. Uchiyama, K. Yamamoto, R. Watanabe, and K. Namba, "Computer-aided diagnosis scheme using a filter bank for detection of microcalcification clusters in mammograms," *IEEE Transactions on Biomedical Engineering*, 53, 273-283, 2006.